J. Am. Soc. Mass Spectrom. (2015) 26:1394–1403
DOI: 10.1007/s13361-015-1144-8

RESEARCH ARTICLE

Base-Pairing Energies of Protonated Nucleoside Base Pairs of dCyd and m^{5}dCyd: Implications for the Stability of DNA *i*-Motif Conformations

Bo Yang, M. T. Rodgers

Department of Chemistry, Wayne State University, Detroit, MI 48202, USA

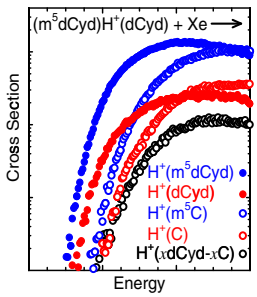

Abstract. Hypermethylation of cytosine in expanded $(CCG)_n$•$(CGG)_n$ trinucleotide repeats results in Fragile X syndrome, the most common cause of inherited mental retardation. The $(CCG)_n$•$(CGG)_n$ repeats adopt *i*-motif conformations that are preferentially stabilized by base-pairing interactions of protonated base pairs of cytosine. Here we investigate the effects of 5-methylation and the sugar moiety on the base-pairing energies (BPEs) of protonated cytosine base pairs by examining protonated nucleoside base pairs of 2′-deoxycytidine (dCyd) and 5-methyl-2′-deoxycytidine (m^{5}dCyd) using threshold collision-induced dissociation techniques. 5-Methylation of a single or both cytosine residues leads to very small change in the BPE. However, the accumulated effect may be dramatic in diseased state trinucleotide repeats where many methylated base pairs may be present. The BPEs of the protonated nucleoside base pairs examined here significantly exceed those of Watson-Crick dGuo•dCyd and neutral dCyd•dCyd base pairs, such that these base-pairing interactions provide the major forces responsible for stabilization of DNA *i*-motif conformations. Compared with isolated protonated nucleobase pairs of cytosine and 1-methylcytosine, the 2′-deoxyribose sugar produces an effect similar to the 1-methyl substituent, and leads to a slight decrease in the BPE. These results suggest that the base-pairing interactions may be slightly weaker in nucleic acids, but that the extended backbone is likely to exert a relatively small effect on the total BPE. The proton affinity (PA) of m^{5}dCyd is also determined by competitive analysis of the primary dissociation pathways that occur in parallel for the protonated (m^{5}dCyd)H$^+$(dCyd) nucleoside base pair and the absolute PA of dCyd previously reported.

Keywords: Base-pairing energies, Density functional theory, 2′-Deoxycytidine, DNA *i*-Motif, Methylation, Proton affinities

Received: 7 January 2015/Revised: 10 March 2015/Accepted: 17 March 2015/Published Online: 22 May 2015

Introduction

The effect of nucleotide modification on DNA is one of the oldest questions in DNA science, and information is still rather limited. Modifications of DNA can occur along the phosphate backbone or to the sugar or nucleobase moieties. Such modifications not only affect the binding affinity and specificity of DNA but also possess pharmacokinetic and toxicological properties for medicinal chemistry [1]. DNA methylation, typically cytosine methylation, is the most common epigenetic modification in eukaryotic genomes that can regulate chromatin status and directly affect the ability of transcription factors to access DNA. Roughly 5% of cytosines in the human genome are methylated, mainly at dinucleotide CpG sites [2], and there is considerable variation in the pattern of methylation with cell type and state [3, 4]. Methylation of cytosine residues can alter the appearance of the major groove of DNA, where DNA binding proteins generally bind. These epigenetic "markers" can be copied after DNA synthesis, leading to heritable changes in chromatin structure. The majority of methylated CpG sites are found in repetitive DNA elements, suggesting that cytosine methylation has evolved as a defense against transposons and other parasitic elements [5]. In somatic cells, promoter methylation often shows a correlation with gene expression: CpG methylation may directly interfere with the binding of certain transcriptional regulators to their cognate DNA sequences or may enable recruitment of methyl-CpG binding proteins that create a repressed chromatin environment

Electronic supplementary material The online version of this article (doi:10.1007/s13361-015-1144-8) contains supplementary material, which is available to authorized users.

Correspondence to: M. T. Rodgers; *e-mail:* mrodgers@chem.wayne.edu

[6]. DNA methylation patterns are highly dysregulated in cancer. Changes in methylation status are required for development [4, 7], and have been postulated to inactivate tumor suppressors and activate oncogenes, thus contributing to tumorigenesis [8] and other disease states [9]. Cytosine methylation is also a major contributor to the generation of disease-causing germline and somatic mutations that cause cancer [10, 11]. Previous studies have shown that Fragile X syndrome is caused by methylation at CpG sites, which may involve 5-methylation of cytosine residues and/or 8-methylation of guanine residues, and may involve CpG sites associated with the protonated cytosine base pairs or distant from them [12–14].

Fragile X syndrome is the most widespread inherited cause of mental retardation in humans, and results in intellectual disabilities and physical deformities [15, 16]. It has previously been shown that the expansion of $(CCG)_n$•$(CGG)_n$ trinucleotide repeats beyond 230 trinucleotides leads to Fragile X syndrome [12–14]. The proposed structure of single $(CCG)_n$ and $(CCG)_n$•$(CGG)_n$ trinucleotide repeat strands involve noncanonical DNA structures such as the DNA *i*-motif that may be the cause of the disease [17–19]. The secondary structure of the DNA *i*-motif is a four-stranded structure consisting of parallel-stranded DNA duplexes zipped together in an anti-parallel orientation by intercalated protonated nucleobase pairs of cytosine (C^+•C) [20]. Recently, studies have shown that the structure of the *i*-motif is conserved in the gas phase when electrospray ionization (ESI) is used as the ionization technique [21], indicating that under favorable conditions, gas-phase studies may indeed provide insight into solution-phase structure and function.

Electronic structure calculations performed at the B3LYP/6-311+G(2d,2p)// B3LYP/6-31G* level of theory predict that the base-pairing energy (BPE) of the protonated nucleoside base pair of 2′-deoxycytidine ($dCyd^+$•dCyd) is 166.8 kJ/mol, whereas BPEs of the protonated nucleobase pair C^+•C and canonical neutral Watson-Crick dGuo•dCyd base pair are 169.7 and 95.8 kJ/mol, respectively, indicating that the 2′-deoxyribose sugar very slightly weakens the base-pairing interactions, but that *i*-motif conformations are still preferentially stabilized by base-pairing interactions of noncanonical protonated $dCyd^+$•dCyd nucleoside base pairs. Given the important biological roles that DNA *i*-motif conformations may play in several human diseases and cancer, including lung carcinoma [22], breast carcinoma [23], and Burkitt's lymphomas [24], a comprehensive study is needed to characterize the influence of methylation on the BPEs. Recently, quantitative determination of the strength of the BPEs of protonated homo- and hetero-nucleobase pairs of cytosine (C), 5-methylcytosine (m^5C), 1-methylcytosine (m^1C), and 1,5-dimethylcytosine (m^{15}_2C) was reported using threshold collision-induced dissociation techniques (TCID) [25–27]. The methyl substituent at the N1 position serves as a mimic for the sugar moiety such that implications for the effects of the 2′-deoxyribose moiety on the BPE are elucidated. In the case of homo-nucleobase pairs, 5-hypermethylation was found to increase the BPE, whereas 1-hypermethylation was found to exert almost no effect on the BPE. Hence, 1,5-dimethylation of both cytosines results in an intermediate increase in the BPE. These results suggest that DNA *i*-motif conformations should be stabilized under 5-hypermethylation conditions. In the case of the hetero-nucleobase pairs, methylation of a single cytosine at the N1, C5, or N1 and C5 positions weakens the BPE, and therefore would tend to destabilize DNA *i*-motif conformations. Whether methylation of cytosine residues will produce similar effects in larger, more biologically relevant model systems is not clear. Therefore, in the present work, we extend our studies to include protonated homo- and hetero-nucleoside base pairs of 2′-deoxycytidine (dCyd) and 5-methyl-2′-deoxycytidine (m^5dCyd) using TCID techniques such that the effects of the 2′-deoxyribose sugar on the BPEs is directly determined. Methylation also affects the proton affinities (PAs) of the nucleosides. Accurate determination of the PAs of nucleosides can yield valuable information regarding the intrinsic nucleoside reactivity and the role of the local environment in affecting nucleoside reactivity. However, very limited thermochemical data has thus far been reported in the literature. The PA of dCyd has been measured and reported [28], whereas no PAs of modified dCyd have been reported. The relative N3 PAs of dCyd and m^5dCyd are obtained from the experimental data via competitive analysis of the two primary dissociation pathways that occur in parallel for the $(m^5dCyd)H^+(dCyd)$ complexes. The absolute N3 PA of m^5dCyd is then obtained using the relative PAs determined here and the PA of dCyd, 988.3 ± 8.0 kJ/mol, reported in the literature [28]. The measured values are compared with theoretical results calculated at the B3LYP level of theory to evaluate the ability of this level of theory for predicting accurate energetics for these protonated nucleoside base pairs.

Experimental and Computation

General Procedures

The energy-dependent CID behavior of three protonated nucleoside base pairs, $(dCyd)H^+(dCyd)$, $(m^5dCyd)H^+(m^5dCyd)$, and $(m^5dCyd)H^+(dCyd)$, is studied using a guided ion beam tandem mass spectrometer that has been described in detail previously [29]. The $(x\text{dCyd})H^+(y\text{dCyd})$ protonated nucleoside base pairs are generated by ESI from solutions containing 0.5–1 mM of dCyd and/or m^5dCyd and 1% (v/v) acetic acid in an approximately 50%:50% MeOH:H_2O mixture. The ions are desolvated, focused, and thermalized in a radio frequency (rf) ion funnel and hexapole ion guide collision cell interface. The thermalized ions emanating from the hexapole ion guide are extracted, accelerated, and focused into a magnetic sector momentum analyzer for mass analysis. Mass-selected $(x\text{dCyd})H^+(y\text{dCyd})$ protonated nucleoside base pairs are decelerated to a desired kinetic energy and focused into a rf octopole ion beam guide that radially traps ions [30–32] such that scattered reactant and products ions are collected efficiently as they drift toward the exit of the octopole. The octopole passes through a static gas cell where the reactant $(x\text{dCyd})H^+(y\text{dCyd})$ protonated nucleoside base pairs undergo

collision-induced dissociation (CID) with Xe [33–35] under nominally single collision conditions, ~0.05–0.10 mTorr. Product and unreacted (*x*dCyd)H^+(*y*dCyd) ions drift to the end of the octopole, where they are focused into a quadrupole mass filter for the second stage of mass analysis. The ions are detected using a secondary electron scintillation detector of the Daly type and standard pulse counting techniques. The nucleosides, dCyd and m^5dCyd, were purchased from Alfa Aesar (Ward Hill, MA, USA).

Theoretical Calculations

The stable low-energy tautomeric conformations of dCyd and H^+(dCyd) have previously been examined by Wu et al. as described in detail elsewhere [36]. In the present study, geometry optimizations and frequency analyses of the low-energy tautomeric conformations of m^5dCyd and H^+(m^5dCyd) were performed using Gaussian 09 [37] at the B3LYP/6-31G* level of theory. Owing to the structural flexibility of the protonated nucleoside base pairs of dCyd and m^5dCyd, simulated annealing was first carried out to search for candidate structures using HyperChem [38] software with the Amber 2 force field. Initial structures of each protonated nucleoside base pair underwent a 300 cycle simulated annealing procedure, with each cycle beginning and ending at 0 K, lasting for 0.8 ps, and achieving a simulation temperature of 1000 K. Heating and cooling times for each cycle were 0.3 ps each, allowing 0.2 ps for the ions to sample conformational space at the simulation temperature. Relative energies were computed using molecular mechanics methods every 0.001 ps. The most stable conformers accessed at the end of each annealing cycle were saved and used to initiate the subsequent cycle. All structures within 30 kJ/mol of the lowest-energy structure found via the simulated annealing procedure, as well as others representative and encompassing the entire range of structures found, were further optimized and frequency analyzed at the B3LYP/6-31G* level of theory. Single point energy calculations for *x*dCyd, H^+(*x*dCyd), and three (*x*dCyd)H^+(*y*dCyd) protonated nucleoside base pairs, where *x*, *y* = H and/or m^5, were performed at the B3LYP/6-311+G(2d,2p) level of theory using B3LYP/6-31G* optimized geometries. Zero-point energy (ZPE) corrections were determined using vibrational frequencies calculated at the B3LYP level of theory and scaled by a factor of 0.9804 [39]. To obtain accurate energetics, basis set superposition error corrections (BSSEs) are also included in the calculated BPEs using the full counterpoise approach [40, 41]. The polarizabilities of the neutral nucleosides, which are required for threshold analyses, are calculated at the PBE1PBE/6-311+G(2d,2p) level of theory. This level of theory has been shown to provide polarizabilities that exhibit better agreement with experimental values than the B3LYP functional employed here for structures and energetics [42].

Thermochemical Analysis

The threshold regions of the measured CID cross sections are modeled using procedures developed elsewhere [43–50] that have been found to reproduce CID cross sections well [25–27, 29, 51–55]. Details regarding data handling and analysis procedures, which include explicitly accounting for the internal and translational energy distributions of the (*x*dCyd)H^+(*y*dCyd) and Xe reactants, the effects of multiple ion-neutral collisions, and the lifetime of the dissociating protonated nucleoside base pairs, are summarized in the Supplementary Information.

Results and Discussion

Cross Sections for Collision-Induced Dissociation

Experimental cross sections were obtained for the interaction of Xe with three (*x*dCyd)H^+(*y*dCyd) protonated nucleoside base pairs, (dCyd)H^+(dCyd), (m^5dCyd)H^+(m^5dCyd), and (m^5dCyd)H^+(dCyd) over the range of collision energies extending from ~0 to 6 eV. The energy-dependent CID cross sections of all three (*x*dCyd)H^+(*y*dCyd) protonated nucleoside base pairs are shown in Figure 1. The primary dissociation pathway observed for the protonated homo-nucleoside base pairs corresponds to cleavage of the three hydrogen bonds responsible for the binding in these species, and resulting in loss of the neutral nucleoside in the CID reactions 1.

$$(x\mathrm{dCyd})\mathrm{H}^+(x\mathrm{dCyd}) + \mathrm{Xe} \rightarrow \mathrm{H}^+(x\mathrm{dCyd}) + x\mathrm{dCyd} + \mathrm{Xe} \quad (1)$$

CID of the (m^5dCyd)H^+(dCyd) protonated hetero-nucleoside pair leads to two primary dissociation pathways that occur in parallel and compete with each other, reactions 2 and 3.

$$(\mathrm{m}^5\mathrm{dCyd})\mathrm{H}^+(\mathrm{dCyd}) + \mathrm{Xe} \rightarrow \mathrm{H}^+(\mathrm{m}^5\mathrm{dCyd}) + \mathrm{dCyd} + \mathrm{Xe} \quad (2)$$

$$(\mathrm{m}^5\mathrm{dCyd})\mathrm{H}^+(\mathrm{dCyd}) + \mathrm{Xe} \rightarrow \mathrm{H}^+(\mathrm{dCyd}) + \mathrm{m}^5\mathrm{dCyd} + \mathrm{Xe} \quad (3)$$

Production of H^+(m^5dCyd) is energetically favored over production of H^+(dCyd), indicating that the N3 PA of m^5dCyd exceeds that of dCyd. Sequential dissociation pathways involving cleavage of the N-glycosidic bonds of the primary products, H^+(dCyd) and H^+(m^5dCyd), via CID reactions 1–3, producing H^+(C), H^+(m^5C), and the protonated 2′-deoxyribityl moiety, H^+(*x*dCyd – *x*C), are also observed at elevated collision energies, reactions 4 and 5.

$$\mathrm{H}^+(x\mathrm{dCyd}) \rightarrow \mathrm{H}^+(x\mathrm{C}) + (x\mathrm{dCyd}{-}x\mathrm{C}) \quad (4)$$

$$\mathrm{H}^+(x\mathrm{dCyd}) \rightarrow \mathrm{H}^+(x\mathrm{dCyd}{-}x\mathrm{C}) + x\mathrm{C} \quad (5)$$

These dissociation behaviors are consistent with previous TCID and IRMPD studies of protonated nucleobase pairs and isolated protonated nucleosides, including H^+(dCyd) [25–27, 36].

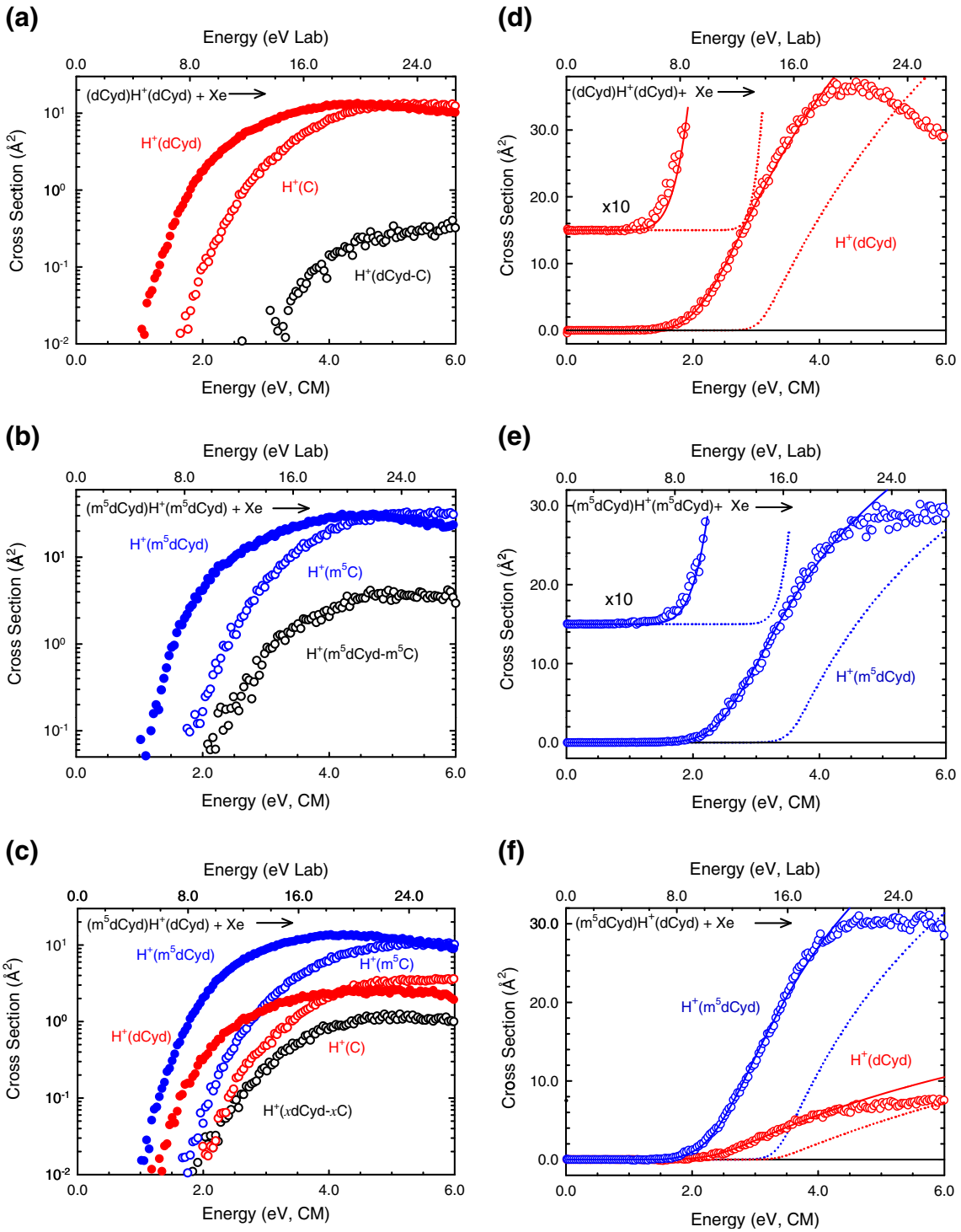

Figure 1. Cross sections for CID of the (dCyd)H$^+$(dCyd), (m^{5}dCyd)H$^+$(m^{5}dCyd), and (m^{5}dCyd)H$^+$(dCyd) protonated nucleoside base pairs with Xe as a function of collision energy in the center-of-mass frame (lower x-axis) and laboratory frame (upper x-axis), (**a**)–(**c**). Data are shown for a Xe pressure of ~0.1 mTorr. Zero-pressure-extrapolated cross sections of the (dCyd)H$^+$(dCyd), (m^{5}dCyd)H$^+$(m^{5}dCyd), and (m^{5}dCyd)H$^+$(dCyd) protonated nucleoside base pairs with Xe in the threshold region as a function of kinetic energy in the center-of-mass frame (lower x-axis) and the laboratory frame (upper x-axis), (**d**)–(**f**). The solid lines show the best fits to the data using the models of Supplementary equations S1 and S2 convoluted over the neutral and ion kinetic and internal energy distributions. The dotted lines show the model cross sections in the absence of experimental kinetic energy broadening for protonated nucleoside base pairs with an internal temperature of 0 K

Theoretical Results

As mentioned in the Theoretical Calculations section, the stable tautomeric conformations of the neutral *x*dCyd and protonated H^+(*x*dCyd) nucleosides as well as the (*x*dCyd)H^+(*y*dCyd) protonated nucleoside base pairs, were examined at the B3LYP/6-31G* level of theory. The structures of the ground-state tautomeric conformations of all three protonated nucleoside base pairs calculated at the B3LYP/6-31G* are shown in Figure 2. To differentiate the various stable low-energy tautomeric conformations of these species, lower case Roman numerals are used to describe the tautomeric conformations of the neutral nucleoside, whereas upper case Roman numerals with a "+" sign are used to describe the tautomeric conformations of the protonated nucleoside, and both are ordered based on the relative Gibbs free energies at 298 K of the low-energy tautomeric conformations of dCyd and H^+(dCyd). As can be seen in the figure, the ground-state structures of all three protonated nucleoside base pairs involve binding via three hydrogen-bonding interactions and adopt an anti-parallel configuration of the protonated and neutral nucleosides, corresponding to the most commonly observed conformation in double-stranded DNAs. In the ground-state structure of the protonated nucleoside base pairs, the excess proton is bound to the N3 atom of the cytosine residue of the protonated nucleoside, H^+(*x*dCyd), which corresponds to the ground-state $\mathbf{I}^+$ conformer of isolated H^+(*x*dCyd). The cytosine and/or 5-methylcytosine nucleobases take on anti-orientations relative to the glycosidic bonds and the sugars are in C3′-endo configurations. The neutral nucleoside, *x*dCyd, also exists as the ground-state **i** conformer in the ground-state structures of the protonated nucleoside base pairs. The orientation of the nucleobase and sugar puckering are highly similar to that of the ground-state $\mathbf{I}^+$ conformer of the protonated nucleoside, H^+(*x*dCyd). The ground-state tautomeric conformation of the protonated nucleoside base pairs is thus designated as **$\mathbf{I}^+$•••i_3a(AC3, AC3)** to indicate that the ground $\mathbf{I}^+$ tautomeric conformation of the protonated nucleoside binds to the ground **i** tautomeric conformation of the neutral nucleoside. The underscore **3a** designation indicates that the binding occurs via three hydrogen-bonding interactions and the protonated and neutral bases are bound in an anti-parallel configuration. The orientation of the nucleobase relative to the glycosidic bond and the sugar puckering for the protonated and neutral nucleosides are indicated in parentheses, respectively. The upper case letter **A** indicates that the nucleobase takes on an anti-orientation, whereas **C3** indicates that the sugar moiety is in a C3′-endo sugar configuration. In the protonated (m^5dCyd)H^+(dCyd) nucleoside base pair, the excess proton preferentially bind to the N3 atom of m^5dCyd, indicating that the N3 proton affinity of m^5dCyd exceeds that of dCyd.

Threshold Analysis

The model of Supplementary Equation S1 was used to analyze the thresholds for reaction 1 for the (dCyd)H^+(dCyd) and (m^5dCyd)H^+(m^5dCyd) nucleoside base pairs, whereas Supplementary Equation S2 was used to analyze the thresholds for

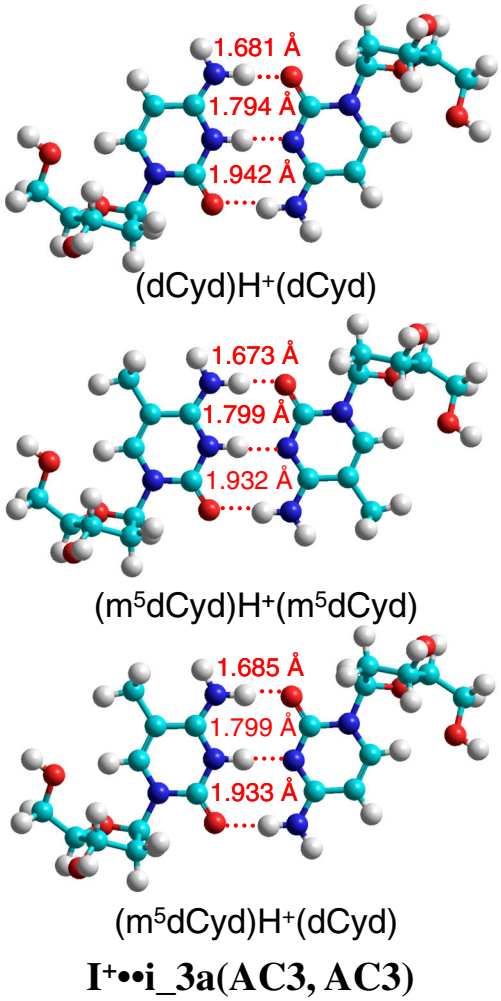

Figure 2. B3LYP/6-31G* optimized geometries of the ground-state **$\mathbf{I}^+$•••i_3a(AC3, AC3)** conformations of the (dCyd)H^+(dCyd), (m^5dCyd)H^+(m^5dCyd), and (m^5dCyd)H^+(dCyd) protonated nucleoside base pairs

reactions 2 and 3 for the (m^5dCyd)H^+(dCyd) nucleoside base pair as described in the Supplementary Information. Based on the computational results, a loose phase space limit transition state (PSL TS) model [48] is applied. The results of these analyses are summarized in Table S3 of the Supplementary Information and shown in Figure 1. The thresholds determined are summarized in Table 1. In all three systems, the experimental cross sections are accurately reproduced using a loose PSL TS model [48]. The relative N3 PAs of dCyd and m^5dCyd are also obtained from competitive analyses of the primary dissociation pathways for the protonated (m^5dCyd)H^+(dCyd) nucleoside base pair. Supplementary Table S3 also includes threshold values, E_0, obtained without inclusion of the RRKM lifetime analysis. Comparison of these results with the E_0(PSL) values provides a measurement of the kinetic shift associated with the finite experimental time window.

Previously, the PA of dCyd was measured using the kinetic method as 988.3 ± 8.0 kJ/mol [28]. Using this value to anchor

Table 1. Base-Pairing Energies of Protonated Nucleobase and Nucleoside Base Pairs at 0 K in kJ/mol[a]

System	TCID	B3LYP[b]	
		D_0	$D_{0,\ BSSE}$[c]
$(dCyd)H^+(dCyd)$	159.8 (5.2)	166.8	163.7
$(m^5dCyd)H^+(m^5dCyd)$	162.0 (5.7)	169.5	166.4
$(m^5dCyd)H^+(dCyd)$	162.6 (5.8)	165.3	162.2
$(C)H^+(C)$	169.9 (4.6)[d]	171.7[d]	168.9[d]
$(m^5C)H^+(m^5C)$	177.4 (5.3)[d]	176.3[d]	173.3[d]
$(m^1C)H^+(m^1C)$	170.7 (5.3)[e]	169.7[e]	166.8[e]
$(m_2{}^{15}C)H^+(m_2{}^{15}C)$	172.3 (5.8)[e]	169.7[e]	166.8[e]
$(m^5C)H^+(C)$	163.6 (5.1)[f]	169.7[f]	166.8[f]
$(m_2{}^{15}C)H^+(m^1C)$	160.9 (4.7)[e]	166.9[e]	164.0[e]
AEU/MAD[g]	5.6 (0.3)	5.7 (2.6)	2.9 (2.2)

[a]Present results, uncertainties are listed in parentheses.
[b]Calculated at the B3LYP/6-311+G(2d,2p) level of theory including ZPE corrections.
[c]Also includes BSSE corrections.
[d]Values taken from reference [27]
[e]Values taken from reference [25].
[f]Values taken from reference [26].
[g]Average experimental uncertainty (AEU). Mean absolute deviation (MAD) between the measured and computed values.

our measurement of the relative N3 PAs of m^5dCyd and dCyd, the N3 PA of m^5dCyd is determined as 994.4 ± 8.4 kJ/mol.

The entropy of activation, $\Delta S^\dagger$, is a measure of the looseness of the TS and also a reflection of the complexity of the system. $\Delta S^\dagger$ is largely determined from the molecular constants used to model the energized complex and the TS, but also depends on the threshold energy, E_0(PSL). The $\Delta S^\dagger$(PSL) values at 1000 K are listed in Supplementary Table S3, and vary between 91 and 96 $J{\bullet}K^{-1}{\bullet}mol^{-1}$ across these systems. The large positive entropies of activation determined result from the fact that while the two neutral hydrogen bonds contribute to the stability, they also conformationally constrain the reactant protonated nucleoside base pairs such that the loose PSL TS is a product-like structure that occurs at the centrifugal barrier for dissociation.

Discussion

Comparison of Experiment and Theory

BPEs of the protonated nucleoside base pairs at 0 K measured here by TCID techniques are summarized in Table 1. Also listed in Table 1 are the BPEs of the protonated nucleoside base pairs calculated at the B3LYP/6-311+G(2d,2p) level of theory, including independent ZPE and BSSE corrections. Excellent agreement is achieved between the measured and B3LYP/6-311+G(2d,2p) calculated BPEs for all three protonated nucleoside base pairs. The mean absolute deviation (MAD) between theory and experiment is 2.9 ± 2.2 kJ/mol. The MAD is smaller than the average experimental uncertainty (AEU) in these values, 5.6 ± 0.3 kJ/mol, suggesting that the B3LYP/6-311+G(2d,2p) level of theory accurately describes the hydrogen-bonding interactions responsible for the binding in these protonated nucleoside base pairs. This behavior is consistent with previous TCID studies on similar protonated nucleobase pairs [25–27].

The absolute N3 PA of dCyd was previously reported as 988.3 ± 8.0 [28], whereas the PA of m^5dCyd is determined here as 994.4 ± 8.4 kJ/mol. Both values are in excellent agreement with the B3LYP/6-311+G(2d,2p) calculated values of 991.6 and 999.6 kJ/mol, respectively.

Influence of Methylation and Sugar Moiety on the N3 PA

The absolute N3 PA of C is reported as 949.9 ± 8.0 kJ/mol in the NIST Webbook [56, 57]. More recently, Lee and coworkers re-measured the PA of C along with that of m^1C as 950 ± 13 and 962 ± 13 kJ/mol, respectively [58]. Using these literature values along with relative PAs determined from TCID studies of protonated nucleobase pairs of C, m^1C, m^5C, and $m_2^{15}C$ and a comprehensive maximum likelihood estimation procedure, we recently reported absolute N3 PAs for these nucleobases, and with improved precision for C and m^1C [25]. The N3 PAs of C, m^1C, m^5C, $m_2^{15}C$ [25], and dCyd [28] thus determined, and m^5dCyd determined here, follow the order: m^5dCyd (994.4 ± 8.4 kJ/mol) > dCyd (988.3 ± 8.0 kJ/mol) > $m_2^{15}C$ (979.9 ± 2.9 kJ/mol) > m^1C (964.7 ± 2.9 kJ/mol) > m^5C (963.2 ± 2.9 kJ/mol) > C (949.9 ± 2.8 kJ/mol). Clearly, 1-methylation, 5-methylation, and the sugar moiety all lead to an increase in the N3 PA of cytosine. The electron-donating properties of the methyl and sugar moieties increase the electron density within the aromatic ring, leading to stabilization of the positive charge associated with the excess proton, consistent with the observed trend in the N3 PAs. The sugar moiety produces a larger effect on the N3 PA than methylation and even dimethylation of cytosine attributable to its much larger polarizability and, therefore, results in more significant stabilization of the positive charge associated with the excess proton. The correlations between the polarizabilities and TCID measured absolute N3 PAs of these systems are shown in Figure 3a. The TCID measured absolute N3 PAs of C, m^1C, m^5C, and $m_2^{15}C$ [25] are also included for comparison. Linear regression fits through the data for C, m^1C, and dCyd as well as the analogous 5-methylated series, m^5C, $m_2^{15}C$, and m^5dCyd are also shown. The absolute N3 PAs of the cytosine nucleobases and nucleosides increase as the polarizabilities of these species increase.

Influence of Methylation and the Sugar Moiety on the BPEs

The measured and calculated BPEs at 0 K of the three protonated (*x*dCyd)H^+(*y*dCyd) nucleoside base pairs measured here are listed in Table 1. Experimentally, the BPEs of all three protonated nucleoside base pairs are equal within experimental uncertainties. In agreement with measured values, theory suggests that 5-methylation of a single cytosine residue exerts almost no effect on the BPE, whereas 5-permethylation leads to a slight increase in the BPE. This behavior is consistent with observations made in previous TCID studies for the analogous

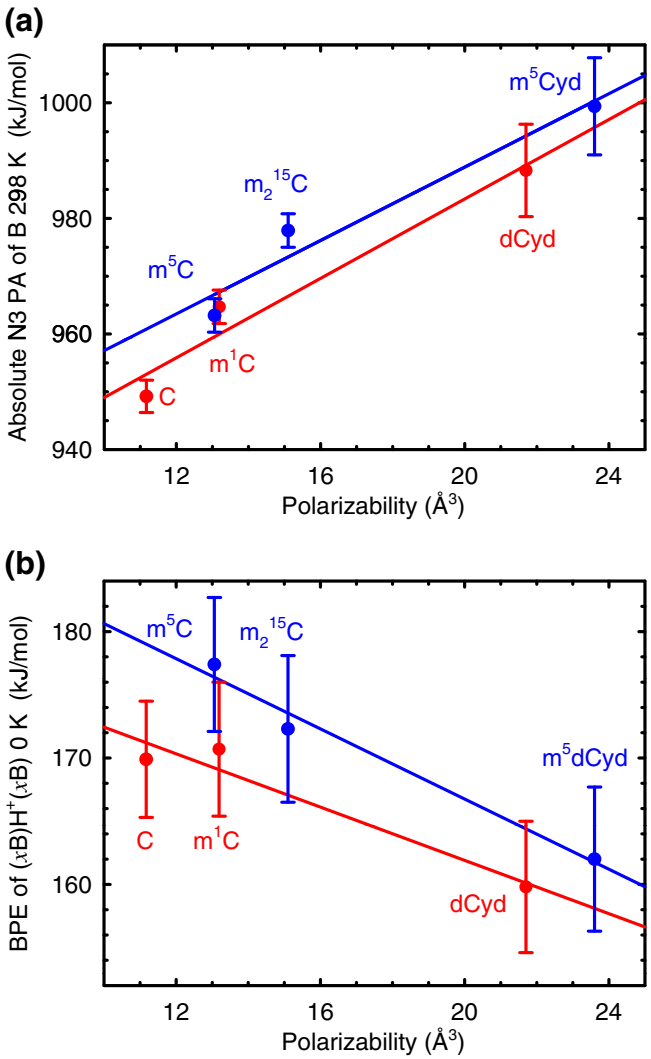

Figure 3. TCID measured absolute N3 PAs of *x*B at 298 K (in kJ/mol) versus calculated polarizability volumes of *x*B, where *x*B = C, m^5C, m^1C, $m_2^{15}C$, dCyd, and m^5dCyd. The N3 PAs of C, m^5C, m^1C, and $m_2^{15}C$ are taken from reference [25], whereas the N3 PA of dCyd is taken from reference [28]. The lines are linear regressions fits to the data for the C, m^1C, and dCyd series, and independently the analogous 5-methylated species, respectively (**a**). TCID measured BPEs of (*x*B)H$^+$(*x*B) at 0 K (in kJ/mol) versus polarizability volumes of *x*B, where *x*B = C, m^5C, m^1C, $m_2^{15}C$, dCyd, and m^5dCyd. The BPEs of (C)H$^+$(C) and (m^5C)H$^+$(m^5C) are taken from reference [27], whereas the BPEs of (m^1C)H$^+$(m^1C) and (m_2^{15}C)H$^+$(m_2^{15}C) are taken from reference [25]. The lines are linear regressions fits to the data for the C, m^1C, and dCyd series, and independently the analogous 5-methylated species, respectively (**b**)

protonated nucleobase pairs of cytosine and 5-methylcytosine [26, 27].

The correlation between the BPEs of the (*x*dCyd)H$^+$(*x*dCyd) nucleoside base pairs measured here and polarizabilities of *x*dCyd is illustrated in Figure 3b. The BPEs of the (C)H$^+$(C), (m^5C)H$^+$(m^5C) [27], (m^1C)H$^+$(m^1C), and (m_2^{15}C)H$^+$(m_2^{15}C) [25] protonated nucleobase pairs measured previously are also included in Table 1 and Figure 3b for comparison. As can be seen in the figure, 5-permethylation of the cytosine residues leads to an increase in the BPEs, but the magnitude of the increase becomes smaller as the polarizability of the nucleobase or nucleoside increases. The BPEs of the protonated nucleoside base pairs also decrease as the polarizabilities of *x*dCyd increase. The BPEs of the (dCyd)H$^+$(dCyd), (m^5dCyd)H$^+$(m^5dCyd), and (m^5dCyd)H$^+$(dCyd) nucleoside base pairs are smaller than those of the corresponding protonated nucleobase pairs, (C)H$^+$(C), (m^5C)H$^+$(m^5C), and (m^5C)H$^+$(C), respectively, indicating that the 2′-deoxyribose sugar leads to a slight decrease in the BPE for of all these protonated nucleoside base pairs. The BPEs of the three protonated nucleoside base pairs are also slightly smaller than those of the corresponding 1-methylated protonated nucleobase pairs, (m^1C)H$^+$(m^1C), (m_2^{15}C)H$^+$(m_2^{15}C), and (m_2^{15}C)H$^+$(m^1C), indicating that the effect of the 2′-deoxyribose sugar on the BPE is parallel, but slightly greater than that of the 1-methyl substituent.

Implications for the Stability of DNA i-Motif Conformations

The base-pairing interactions in the protonated nucleobase pairs of cytosine are the major forces responsible for stabilization of DNA *i*-motif conformations. Previous TCID studies of protonated nucleobase pairs of cytosine and methylated cytosines found that 5-hypermethylation increases the BPE, whereas 1-hypermethylation exerts almost no effect on the BPE. Hence, 1,5-dimethylation of both cytosines results in an intermediate increase in the BPE [25, 27]. These results suggest that DNA *i*-motif conformations should be stabilized under 5-hypermethylation conditions. As mentioned in the Introduction, methylation may also occur at cytosine residues associated with the protonated cytosine base pairs or distant from them as well as at guanine residues of the CpG sites of the trinucleotide repeats. As for 1-methylation of cytosine residues, 5-methylation of cytosine residues not involved in the protonated cytosine base pairs or 8-methylation of guanine residues being distant from the protonated cytosine base pairs should exert an even smaller, and probably a negligible, effect on the BPEs. These results also suggest that hypermethylation of CCG repeats, which is the cause of Fragile-X syndrome, likely occurs to both further stabilize *i*-motif conformations (5-methylation of cytosine residues involved in the protonated cytosine base pairs) and to alter the appearance of the major and minor grooves (5-methylation of cytosine and 8-methylation of guanine residues) and thus alter interactions with DNA binding proteins [12–14]. In the case of the hetero-nucleobase pairs, methylation of a single cytosine at the N1, C5, or N1 and C5 positions very slightly weakens the BPE and, therefore, would tend to very slightly destabilize DNA *i*-motif conformations, but such isolated modifications should produce a negligible effect on the

overall stability [25, 26]. In the present TCID studies of protonated nucleoside base pairs, 5-methylation of a single or both cytosine residues exerts almost no effect on the BPE and, thus, should produce a very minor effect on the stability of DNA *i*-motif conformations. In agreement with experimental observations, theory also suggests that the effects of methylation on the BPE are small. Theoretically, 5-permethylation of cytosine residues slightly increases the BPEs, whereas 5-methylation of a single cytosine residue leads to a small decrease in the BPE. However, the BPEs of all of the (*x*dCyd)H^+(*y*dCyd) protonated nucleoside pairs are still much greater than those of canonical Watson-Crick G•C and dGuo•dCyd and neutral C•C and dCyd•dCyd base pairs, suggesting that DNA *i*-motif conformations are still favored over conventional base pairing. Thus, although theory suggests that 5-methylation of a single cytosine residue tends to weaken the base-pairing interactions in the nucleoside pairs, the effects are sufficiently small that *i*-motif conformations should be stable to such modifications. Even though the change in the BPE induced by methylation is not large for a single nucleoside pair, the accumulated effect can be dramatic in diseased state trinucleotide repeats associated with the Fragile X syndrome where more than 230 trinucleotides and hundreds of 5-methylated cytosine base pairs may be present. Because methylation at different positions may lead to an increase or decrease in the BPE, the overall influence of methylation will be seen in the number of trinucleotide repeats required to cause structural conversion from canonical Watson-Crick base-pairing to DNA *i*-motif conformations.

To further probe the influence of modifications on the stability of DNA *i*-motif conformations, other factors that play roles in stabilizing/destabilizing these noncanonical structures such as nucleobase-stacking interactions and the folding of the nucleic acid strands must also be considered. Follow-up work to examine how these base-pairing interactions evolve in increasingly larger model systems including the analogous protonated pairs of the 2′-deoxycytidine nucleotides and extending to $(CCG)_n$ trinucleotide repeats that are associated with the formation of *i*-motif conformations and Fragile X syndrome are being pursued. The present results show that the B3LYP level of theory provides accurate estimates for the energetics of binding in protonated nucleoside base pairs and, therefore, may be suitable for investigating larger and increasingly biologically relevant model systems. The present studies also show that epigenetic 5-methylation of cytosine exerts a stabilizing influence in the presence of the 2′-deoxyribose sugar moiety and would tend to stabilize DNA *i*-motif conformations, thereby requiring fewer trinucleotide repeats for structural conversion of Watson-Crick base paired DNA to *i*-motif conformations. Information provided by this work, including structures, the energy-dependent dissociation behavior, and relative stabilities of these protonated nucleoside base pairs should also facilitate experiments and data interpretation for studies of larger and increasingly biologically relevant model systems.

Conclusions

In order to elucidate the effects of the 2′-deoxyribose sugar on the base-pairing interactions in protonated cytosine base pairs as well as the effects of 5-methylation in the presence of the sugar moiety, the threshold collision-induced dissociation behavior of three protonated nucleoside base pairs, (dCyd)H^+(dCyd), (m^5dCyd)H^+(m^5dCyd), and (m^5dCyd)H^+(dCyd), are examined in a guided ion beam tandem mass spectrometer. The primary dissociation pathway observed for the protonated nucleoside base pairs corresponds to cleavage of the three hydrogen bonds responsible for the binding in these complexes, resulting in loss of the neutral nucleoside. For CID of the hetero-nucleoside base pairs, both protonated nucleosides are observed in competition. Thresholds corresponding to BPEs are determined after careful consideration of the effects of the kinetic and internal energy distributions of the (*x*dCyd)H^+(*y*dCyd) and Xe reactants, multiple collisions with Xe, and the lifetime of the activated (*x*dCyd)H^+(*y*dCyd) complexes using a loose PSL TS model. Competitive threshold analysis of the two dissociation pathways that occur in parallel for the hetero-nucleoside base pair provides the relative N3 PA of 2′-deoxycytidine and 5-methyl-2′-deoxycytidine, which are put on an absolute scale using the PA of dCyd previously reported. Theoretical estimates for the BPEs of the (*x*dCyd)H^+(*y*dCyd) complexes and the N3 PA of m^5dCyd are also determined from calculations performed at the B3LYP/6-311+G(2d,2p) level of theory. Excellent agreement between experimental and theoretical BPEs and absolute and relative N3 PAs of dCyd and m^5dCyd is found for the B3LYP level of theory. 5-Methylation of cytosine residues produces a very minor effect on the strength of the base-pairing interactions in the protonated nucleoside base pairs and, thus, should exert a very minor effect on the stability of DNA *i*-motif conformations. The BPEs of the protonated nucleoside base pairs are slightly smaller than those of the corresponding protonated nucleobase pairs, indicating that the 2′-deoxyribose sugar very slightly weakens the base-pairing interactions. The BPEs of the three protonated nucleoside pairs are also slightly smaller than those of the corresponding 1-methylated protonated nucleobase pairs, indicating that the effect of the 2′-deoxyribose sugar on the BPE slightly exceeds that of the 1-methyl substituent. Even though the change in the BPE induced by 5-methylation is rather small for a single nucleoside base pair, the accumulated effect can be dramatic in diseased state trinucleotide repeats where more than 230 trinucleotides and hundreds of protonated 5-methylcytosine base pairs may be present. The BPEs of the protonated nucleoside base pairs examined here significantly exceed those of canonical G•C and dGuo•dCyd and neutral C•C and dCyd•dCyd base pairs, suggesting that the effects of 5-methylation are not sufficient to significantly alter the stability of DNA *i*-motif conformations, but may alter the number of trinucleotide repeats required to induce structural conversion from canonical Watson-Crick base-pairing in double-stranded DNA to DNA *i*-motif conformations. Methylation also affects the N3 PA of cytosine. The N3 PAs of cytosine, methylated cytosines, dCyd, and m^5dCyd follow the order: m^5dCyd >

dCyd > m^{15}_2C > m^1C > m^5C > C, indicating that methylation and the sugar moiety increase the N3 PA in proportion to their effect on the polarizability. The effect of 5-methylation of dCyd is consistent with previous observations for the methylated cytosines, indicating that conclusions of these model studies are robust and should also hold for individual trinucleotides and large nucleic acids relevant to the diseased states of interest [25].

Acknowledgments

Financial support for this work was provided by the National Science Foundation, grant CHE-1409420. The authors thank Wayne State University C&IT for computer time. B.Y. also gratefully acknowledges support from Wayne State University Thomas C. Rumble Graduate and Summer Dissertation Fellowships.

References

1. Crooke, S.T., Bennett, C.F.: Progress in antisense oligonucleotide therapeutics. Annu. Rev. Pharmacol. Toxicol. **36**, 107–129 (1996)
2. Ehrlich, M., Wang, R.Y.: 5-methylcytosine in eukaryotic DNA. Science **212**, 1350–1357 (1981)
3. Lister, R., Ecker, J.R.: Finding the fifth base: Genome-wide sequencing of cytosine methylation. Genome Res. **19**, 959–966 (2009)
4. Lister, R., Pelizzola, M., Dowen, R.H., Hawkins, R.D., Hon, G., Tonti-Filippini, J., Nery, J.R., Lee, L., Ye, Z., Ngo, Q.M., Edsall, L., Antosiewicz-Bourget, J., Stewart, R., Ruotti, V., Millar, A.H., Thomson, J.A., Ren, B., Ecker, J.R.: Human DNA methylomes at base resolution show widespread epigenomic differences. Nature **462**, 315–322 (2009)
5. Goll, M.G., Bestor, T.H.: Eukaryotic cytosine methyltransferases. Annu. Rev. Biochem. **74**, 481–514 (2005)
6. Bird, A.: DNA methylation patterns and epigenetic memory. Gene. Dev. **16**, 6–21 (2002)
7. Meissner, A., Mikkelsen, T.S., Gu, H., Wernig, M., Hanna, J., Sivachenko, A., Zhang, X., Bernstein, B.E., Nusbaum, C., Jaffe, D.B., Gnirke, A., Jaenisch, R., Lander, E.S.: Genome-scale DNA methylation maps of pluripotent and differentiated cells. Nature **454**, 766–770 (2008)
8. Gal-Yam, E.N., Saito, Y., Egger, G., Jones, P.A.: Cancer epigenetics: Modifications, screening, and therapy. Annu. Rev. Med. **59**, 267–280 (2008)
9. Brena, R.M., Huang, T.H., Plass, C.: Quantitative assessment of DNA methylation: Potential applications for disease diagnosis, classification, and prognosis in clinical settings. J. Mol. Med. **84**, 365–377 (2006)
10. Cooper, D.N., Youssoufian, H.: The CpG dinucleotide and human genetic disease. Hum. Genet. **78**, 151–155 (1988)
11. Rideout III, W.M., Coetzee, G.A., Olumi, A.F., Jones, P.A.: 5-methylcytosine as an endogenous mutagen in the human LDL receptor and p53 Genes. Science **249**, 1288–1290 (1990)
12. Sutcliffe, J.S., Nelson, D.L., Zhang, F., Pieretti, M., Caskey, C.T., Saxe, D., Warren, W.T.: DNA methylation represses *FMR-1* transcription in Fragile X syndrome. Hum. Mol. Genet. **1**, 397–400 (1992)
13. Oberlé, I., Rousseau, F., Heitz, D., Kretz, C., Devys, D., Hanauer, A., Boué, J., Bertheas, M.F., Mandel, J.L.: Instability of a 550-base pair DNA segment and abnormal methylation in Fragile X syndrome. Science **252**, 1097–1102 (1991)
14. Pieretti, M., Zhang, F., Fu, Y.-H., Warren, S.T., Oostra, B.A., Caskey, C.T., Nelson, D.L.: Absence of expression of the *FMR-1* gene in Fragile X syndrome. Cell **66**, 817–822 (1991)
15. McLenan, Y., Polussa, J., Tassone, F., Hagerman, R.: Fragile X syndrome. Curr Genom **12**, 216–224 (2011)
16. Garber, K.B., Visootsak, J., Warren, S.T.: Fragile X syndrome. Eur. J. Hum. Genet. **16**, 666–672 (2008)
17. Darlow, J.M., Leach, D.R.F.: Secondary structure in d(CGG) and d(CCG) repeat tracts. J. Mol. Biol. **275**, 3–16 (1998)
18. Mitas, M.: Trinucleotide repeats associated with human disease. Nucleic Acids Res. **25**, 2245–2253 (1997)
19. Fotjík, P., Vorlícková, M.: The Fragile X chromosome (GCC) repeat folds into a DNA tetraplex at neutral pH. Nucleic Acids Res. **29**, 4684–4690 (2001)
20. Gehring, K., Leroy, J.-L., Guéron, M.: A tetrameric DNA structure with protonated cytosine–cytosine base pairs. Nature **363**, 561–565 (1993)
21. Rosu, F., Gabelica, V., Joly, L., Grégoire, G., Pauw, E.D.: Zwitterionic *i*-Motif structures are preserved in DNA negatively charged ions produced by electrospray mass spectrometry. Phys. Chem. Chem. Phys. **12**, 13448–13454 (2010)
22. Little, C.D., Nau, M.M., Carney, D.N., Gazdar, A.F., Minna, J.D.: Amplification and expression of the c-myc oncogene in human lung cancer cell lines. Nature **306**, 194–196 (1983)
23. Munzel, P., Marx, D., Kochel, H., Schauer, A., Bock, K.W.: Genomic alterations of the c-myc protooncogene in relation to the overexpression of c-erbB2 and Ki-67 in human breast and cervix carcinomas. J. Cancer Res. Clin. Oncol. **117**, 603–607 (1991)
24. Clark, H.M., Yano, T., Otsuki, T., Jaffe, E.S., Shibata, D., Raffeld, M.: Mutations in the coding region of c-myc in AIDS-associated and other aggressive lymphomas. Cancer Res. **54**, 3383–3386 (1994)
25. Yang, B., Moehlig, A.R., Frieler, C.E., Rodgers, M.T.: Base-pairing energies of protonated nucleobase pairs and proton affinities of 1-methylated cytosines: Model systems for the effects of the sugar moiety on the stability of DNA *i*-motif conformations. J. Phys. Chem. B. **119**, 1857–1868 (2015)
26. Yang, B., Rodgers, M.T.: Base-pairing energies of proton-bound heterodimers of cytosine and modified cytosines: Implications for the stability of DNA i-Motif conformations. J. Am. Chem. Soc. **136**, 282–290 (2014)
27. Yang, B., Wu, R.R., Rodgers, M.T.: Base-pairing energies of proton-bound homodimers determined by guided ion beam tandem mass spectrometry: Application to cytosine and 5-substituted cytosines. Anal. Chem. **85**, 11000–11006 (2013)
28. Armentano, D., De Munno, G., Di Donna, L., Sindona, G., Giorgi, G., Salvini, L., Napoli, A.: Self-assembling of cytosine nucleoside into triply-bound dimers in acid media. A comprehensive evaluation of proton-bound pyrimidine nucleosides by electrospray tandem mass spectrometry, X-rays diffractometry, and theoretical calculations. J. Am. Soc. Mass Spectrom. **15**, 268–279 (2004)
29. Rodgers, M.T.: Substituent effects in the binding of alkali metal ions to pyridines studied by threshold collision-induced dissociation and ab initio theory: The methylpyridines. J. Phys. Chem. A **105**, 2374–2383 (2001)
30. Teloy, E., Gerlich, D.: Integral cross sections for ion-molecule reactions I. The guided ion beam technique. Chem. Phys. **4**, 417–427 (1974)
31. Gerlich, D.: Inhomogeneous rf Fields: A Versatile Tool for the Study of Processes with Slow Ions. Diplomarbeit [Thesis], University of Freiburg: Federal Republic of Germany (1971)
32. Gerlich, D.: In state-selected and state-to-state ion-molecule reaction dynamics, Part I, Experiment; Ng, C.-Y., Baer, M. (eds.) Adv. Chem. Phys. **82**, 1–176 (1992)
33. Dalleska, N.F., Honma, K., Armentrout, P.B.: Stepwise solvation enthalpies of protonated water clusters: Collision-induced dissociation as an alternative to equilibrium studies. J. Am. Chem. Soc. **115**, 12125–12131 (1993)
34. Aristov, N., Armentrout, P.B.: Collision-induced dissociation of vanadium monoxide ion. J. Phys. Chem. **90**, 5135–5140 (1986)
35. Hales, D.A., Armentrout, P.B.: Effect of internal excitation on the collision-induced dissociation and reactivity of Co_2^+. J. Clust. Sci. **1**, 127–142 (1990)
36. Wu, R.R., Yang, B., Berden, G., Oomens, J., Rodgers, M.: N3 and O2 protonated tautomeric conformations of 2′-deoxycytidine and cytidine co-exist in the gas phase. J. Phys. Chem. B. **119**, 5773–5784 (2015)
37. Frisch, M.J., Trucks, G.W., Schlegel, H.B., Scuseria, G.E., Robb, M.A., Cheeseman, J.R., Scalmani, G., Barone, V., Mennucci, B., Petersson, G.A., Nakatsuji, H., Caricato, M., Li, X., Hratchian, H.P., Izmaylov, A.F., Bloino, J., Zheng, G., Sonnenberg, J.L., Hada, M., Ehara, M., Toyota, K., Fukuda, R., Hasegawa, J., Ishida, M., Nakajima, T., Honda, Y., Kitao, O., Nakai, H., Vreven, T., Montgomery, Jr., J.A., Peralta, J.E., Ogliaro, F., Bearpark, M., Heyd, J.J., Brothers, E., Kudin, K.N., Staroverov, V.N., Kobayashi, R., Normand, J., Raghavachari, K., Rendell, A., Burant, J.C., Iyengar, S.S.,Tomasi, J., Cossi, M., Rega, N., Millam, J.M., Klene, M., Knox, J.E., Cross, J.B., Bakken,V., Adamo, C., Jaramillo, J., Gomperts, R., Stratmann, R.E., Yazyev, O., Austin, A.J., Cammi, R., Pomelli, C., Ochterski, J.W., Martin, R.L., Morokuma, K., Zakrzewski, V.G., Voth, G.A., Salvador, P., Dannenberg, J.J., Dapprich, S., Daniels, A.D., Farkas, Ö., Foresman, J.B., Ortiz, J.V., Cioslowski, J., Fox, D.J.: Gaussian 09, Revision A.1, Gaussian, Inc., Wallingford CT (2009)

38. HyperChem Computational Chemistry Software Package, version 5.0, Hypercube Inc., Gainsville, FL (1997)
39. Exploring Chemistry with Electronic Structures Methods, 2nd Ed., Foresman, J.B., Frisch, Æ. Gaussian Inc., Pittsburg, PA, p.64 (1996)
40. Boys, S.F., Bernardi, R.: Calculation of small molecular interactions by differences of separate total energies—some procedures with reduced errors. Mol. Phys. **19**, 553–566 (1979)
41. van Duijneveldt, F.B., van Duijneveldt-van de Rijdt, J.G.C.M., van Lenthe, J.H.: State of the art in counterpoise theory. Chem. Rev. **94**, 1873–1885 (1994)
42. Smith, S.M., Markevitch, A.N., Romanov, D.A., Li, X., Levis, R.J., Schlegel, H.B.: Static and dynamic polarizabilities of conjugated molecules and their cations. J. Phys. Chem. A. **108**, 11063–11072 (2004)
43. Muntean, F., Armentrout, P.B.: Guided ion beam study of collision-induced dissociation dynamics: Integral and differential cross sections. J. Chem. Phys. **115**, 1213–1228 (2001)
44. Beyer, T.S., Swinehart, D.S.: Number of multiply-restricted partitions [A1]. Commun. ACM **16**, 379 (1973)
45. Stein, S.E., Rabinovitch, B.S.: Accurate evaluation of internal energy level sums and densities including anharmonic oscillators and hindered rotors. J. Chem. Phys. **58**, 2438–2445 (1973)
46. Stein, S.E., Rabinovitch, B.S.: On the use of exact state counting methods in RRKM rate calculations. Chem. Phys. Lett. **49**, 183–188 (1977)
47. Khan, F.A., Clemmer, D.E., Schultz, R.H., Armentrout, P.B.: Sequential bond energies of $Cr(CO)_x^+$, $x = 1–6$. J. Phys. Chem. **97**, 7978–7987 (1993)
48. Rodgers, M.T., Ervin, K.M., Armentrout, P.B.: Statistical modeling of collision-induced dissociation thresholds. J. Chem. Phys. **106**, 4499–4508 (1997)
49. Chesnavich, W.J., Bowers, M.T.: Theory of translationally driven reactions. J. Phys. Chem. **83**, 900–905 (1979)
50. Rodgers, M.T., Armentrout, P.B.: Statistical modeling of competitive threshold collision-induced dissociation. J. Chem. Phys. **109**, 1787–1800 (1998)
51. Chen, Y., Rodgers, M.T.: Structural and energetic effects in the molecular recognition of acetylated amino acids by 18-Crown-6. J. Am. Soc. Mass Spectrom. **23**, 2020–2030 (2012)
52. Austin, C.A., Chen, Y., Rodgers, M.T.: Alkali metal cation–cyclen complexes: Effects of alkali metal cation size on the structure and binding energy. Int. J. Mass Spectrom. **330**, 27–34 (2012)
53. Armentrout, P.B., Yang, B., Rodgers, M.T.: Metal cation dependence of interactions with amino acids: Bond energies of Rb^+ and Cs^+ to Met, Phe, Tyr, and Trp. J. Phys. Chem. B **117**, 3771–3781 (2013)
54. Nose, H., Chen, Y., Rodgers, M.T.: Energy-resolved collision-induced dissociation studies of 1,10-phenanthroline complexes of the late first-row divalent transition-metal cations: Determination of the third sequential binding energies. J. Phys. Chem. A **117**, 4316–4330 (2013)
55. Nose, H., Rodgers, M.T.: Energy-resolved collision-induced dissociation studies of 2,2′-bipyridine complexes of the late first-row divalent transition-metal cations: Determination of the third sequential binding energies. ChemPlusChem **78**, 1109–1123 (2013)
56. Hunter, E.P., Lias, S.G.: Evaluated gas phase basicities and proton affinities of molecules: an update. J. Phys. Chem. Ref. Data **27**, 413–656 (1998)
57. Available at: NIST Chemistry Webbook, http://webbook.nost.gov/chemistry/. Accessed 16 Dec 2014
58. Liu, M., Li, T., Amegayibor, S., Cardoso, D.S., Fu, Y., Lee, J.K.: Gas phase thermochemical properties of pyrimidine nucleobases. J. Org. Chem. **73**, 9283–9291 (2008)